

1 **Design of functional multicomponent liquid crystalline mixtures**
2 **with nano-scale pitch fulfilling deformed helix ferroelectric mode**
3 **demands**

4
5 Katarzyna Kurp¹, Michał Czerwiński^{1*}, Marzena Tykarska¹, Peter Salamon², Alexej Bubnov³

6
7 ¹*Institute of Chemistry, Military University of Technology, Gen. W. Urbanowicza str. 2, 00-908*
8 *Warsaw, Poland*

9 ²*Wigner Research Centre for Physics, Hungarian Academy of Sciences, Budapest, P.O.Box 49,*
10 *H-1525, Hungary*

11 ³*Institute of Physics, The Czech Academy of Sciences, Na Slovance 1999/2, 182 21 Prague,*
12 *Czech Republic*

13
14
15 ***Author for correspondence:**

16 Michał Czerwiński
17 Faculty of Advanced Technologies and Chemistry
18 Military University of Technology
19 Gen. W. Urbanowicza Str. 2, 00-908 Warsaw, Poland
20 Tel +48 261837235
21 Fax. +48 261839582
22 e-mail: michal.czerwinski@wat.edu.pl

23
24 **Running Head:** Design of ferroelectric liquid crystalline mixtures

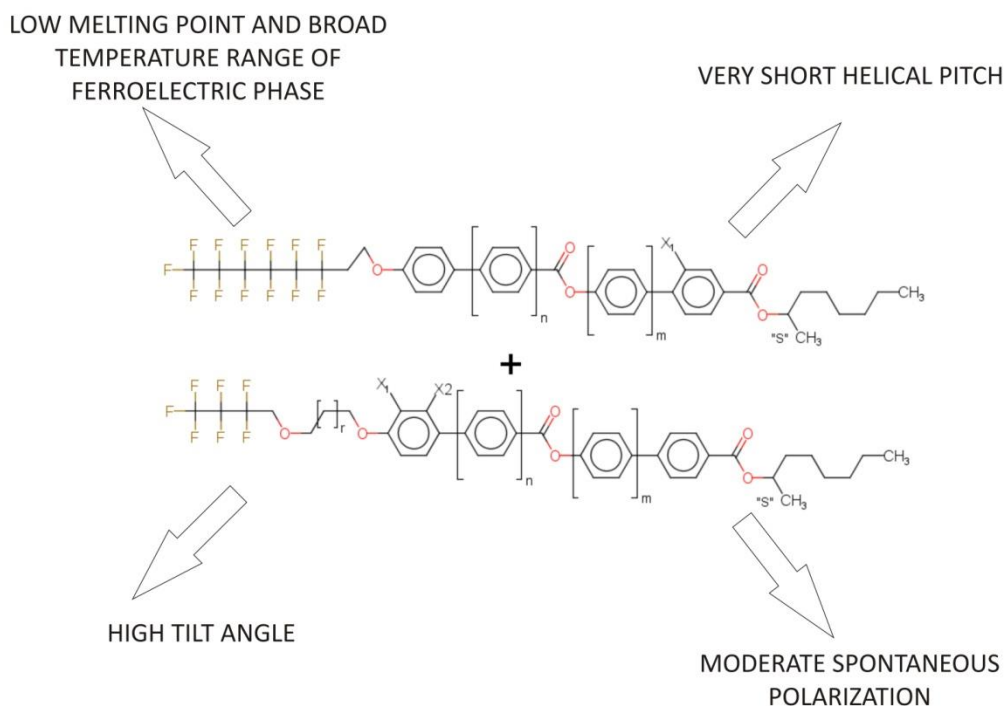
25
26 **Keywords:** ferroelectric liquid crystal; multicomponent mixture; polar smectic phase; helical
27 pitch; phase diagram; self-assembling behaviour; deformed helix ferroelectric mode

1 **Abstract**

2 Design of new functional smectic liquid crystalline mixtures possessing polar behaviour remains
3 quite highlighted task as those materials are highly requested by industry for specific applications
4 in photonics. This work is devoted to specific practical method devoted to design of functional
5 multicomponent ferroelectric liquid crystalline (FLC) mixtures based on chiral components
6 exhibiting the ferroelectric and antiferroelectric polar order. The self-assembling behaviour, tilt
7 angle, spontaneous polarization as well as dielectric properties of the prepared mixtures have been
8 studied and discussed. The three resulting mixtures exhibit a broad range of the ferroelectric
9 smectic phase, very low melting point, short helical pitch (below 180 nm) and relatively high tilt
10 angle (about 40 degree). Excellent chemical stability and compatibility of components as well as
11 moderate values of spontaneous polarization add another great deal to these FLCs materials for
12 application in *deformed helix ferroelectric* mode in photonics and opto-electronics.

13
14
15
16
17
18

16 **Graphical abstract**



19
20
21

1 1. Introduction

2 It is difficult to overestimate the impact of the self-assembling materials on advances of the
3 modern science and technology [1, 2]. Chiral liquid crystals (LC) represent a specific class of
4 organic materials, built up from the rod-like molecules, exhibiting self-orientation, which is
5 possible to drive by an external stimulus like electric or magnetic field, light irradiation, and by
6 mechanical stress. The presence of a polar layered ferroelectric or antiferroelectric structure of
7 nanometre dimensions, characteristic to chiral LC materials, supplies the source of functionality
8 and specific physical properties [2]. Advanced molecular design of new chiral structures can be
9 a very influential and powerful tool to reach the properties desired by specific applications in opto-
10 electronics and photonics. Specifically, the intermolecular interactions liable for the self-
11 assembling can be precisely adjusted by building up the molecules from various units [3-9] or by
12 design of binary/multicomponent mixtures [10-13] or preparation of new LC nanocomposite
13 materials [14-17].

14 Ferroelectric liquid crystals (FLC) fascinated many researchers all over the world for
15 almost three last decades, in particular since N.A. Clark and S.T. Lagerwall demonstrated in 1980
16 [18] the fast switching electro-optical effect (SSFLC-Surface Stabilized Ferroelectric Liquid
17 Crystals) based on the properties related to ferroelectric polar smectic structure. FLCs are very
18 promising competitors of nematic liquid crystals due to their faster response times with a
19 reasonably lower driving voltage. During recent years, FLC materials are still extensively studied
20 [5-9, 12-13, 19-22]. However, especially for photonic applications, the very important
21 continuously tuneable threshold-free phase shift is not offer by the SSFLC effect. In this case,
22 *deformed helix ferroelectric* (DHF) liquid crystals mode is very promising because of tuneable,
23 continuous and hysteresis-free optical phase shift at low voltages and short response time [23-31]
24 either in transmission or in reflection mode [32]. The DHF effect appears in chiral LC materials
25 forming a helical structure. The helix axis is parallel to the substrates' plane of electro-optical cell
26 and it is tilted after applying electric field E (which should be lower than the critical field E_C of
27 the helix unwinding). The transmission (T), switching time (τ) and critical electric field (E_C), which
28 characterize DHF mode, can be described by the following equations [31]:

$$29 \quad T_h = \sin^2 2[\beta \pm \Delta\alpha(E)] \cdot \sin^2 \frac{\pi d_{FLC} \Delta n_{eff}(\lambda, f, E)}{\lambda} \quad (1)$$

$$30 \quad \tau = \frac{\gamma_\phi p_0^2}{K4\pi^2} \quad (2)$$

$$31 \quad E_C = \frac{\pi^4}{4} \frac{K}{P_S p_0^2} \quad (3)$$

1 where: β is the angle between the polarizer and helix axis of the ferroelectric phase; $\Delta\alpha$ denotes
2 the shift of helical axis due to electric field; Δn_{eff} is the effective birefringence and λ is the
3 wavelength; γ_φ is the rotation viscosity; K is the elastic constant, p_o is the helical pitch length; P_s
4 is the spontaneous polarization. From equations (1-3) it is clearly follow that one of the most
5 important material parameter (as it strongly affects τ and E_C in DHF) is the helical pitch length,
6 which should be as low as possible (at least below 200 nm). High tilt angle (ideally as close to 45
7 degrees as possible) promoting high transmission and a moderate spontaneous polarization (ideally
8 within range 120-180 nC/cm²) are further very important and required features. This is truly so as
9 on the one hand low values of spontaneous polarization results in a strong decrease of contrast,
10 and on the other hand high P_s values cause the shortening of electric field range in which DHF
11 effect appears.

12 Recently, an alternative method [33] to obtain FLC materials responding the requirements
13 of DHF mode has been shown. It is based on smart mixing of exclusively chiral compounds in a
14 specific proportion in which the competition and frustration between the ferroelectric and
15 antiferroelectric polar order exists and that in turns is beneficial for obtaining V-shape electro-
16 optical switching [34, 35] (important feature in DHF mode). Due to that we obtained the best
17 mixture (with acronym **W-212B3A**) with almost appropriate properties but exhibiting also two
18 specific disadvantages that are still needed to be resolved. The first one is associated with a
19 possible instability that might occur in a mixture based on components with different molecular
20 structure. Another one is too high values of spontaneous polarization which, according to equation
21 (3), considerably decrease the value of E_C . Furthermore, our basic research [3] confirms that two
22 ring compounds with a very low melting point and the absence of any liquid crystalline behaviour
23 can effectively decrease the helical pitch while mixing with FLC materials. On the other hand, two
24 ring compounds exhibiting the SmA* phase cause unwinding of the helix in FLCs [3].

25 The main objective of this work is to achieve optimum effectiveness of DHF effect by
26 design of several new ferroelectric liquid crystalline mixtures, based on the method described
27 above. The designed mixtures are expected (i) to fulfil almost all material requirements for DHF
28 mode and (ii) to be consisted of structurally similar compounds that can cause the required
29 tunability of spontaneous polarization and helical pitch length values.

30

31 **2. Experimental**

32 The phase transition sequence was determined from the textures and their changes on
33 planar cells (where the long axes of molecules are oriented parallel to the substrates), using
34 polarizing optical microscope (Nikon Eclipse E600POL, Nikon, Tokyo, Japan). The planar cells
35 (AWAT company, Warsaw, Poland) in bookshelf geometry (where the smectic molecular layers

1 are oriented uniformly) for texture observations and electro-optical studies were made from glass
2 with transparent electrodes of indium-tin-oxide (ITO) ($5 \times 5 \text{ mm}^2$), separated by Mylar[®] sheets
3 defining the cell thickness ($12 \text{ }\mu\text{m}$ thick). The sample cells were filled with the studied FLC
4 mixtures in the isotropic phase by the capillary action. The Linkam LTS E350 (Linkam, Tadworth,
5 UK) heating/cooling stage equipped with a TMS 93 temperature controller was used, enabling
6 temperature stabilization within $\pm 0.1 \text{ }^\circ\text{C}$. Dependencies of phase transition temperatures upon
7 mass fraction of components are presented.

8 The measurements of the spontaneous polarization, tilt angle as well as switching ON time
9 (τ_{10-90}) have been done on similar planar samples. Values of the spontaneous polarization, P_s , have
10 been determined from the current measurements with a triangular electric field switching at a
11 frequency of 50 Hz and an applied electric field magnitude of $20 \text{ V}/\mu\text{m}$. A specific software for
12 automation of the spontaneous polarization measurements has been developed and used. Tilt angle,
13 θ_s , has been determined optically under the applied d.c. electric field $\pm 10 \text{ V}/\mu\text{m}$, by measuring the
14 angular difference between the extinction positions of the unwound structures under fields of
15 opposite polarity. Values of the spontaneous polarization, tilt angle and switching ON time have
16 been measured on cooling.

17 The helical pitch measurements were performed based on the selective light reflection
18 phenomenon. Before measurements, a thin layer of orienting surfactant was applied on the glass
19 plate to force the required homeotropic alignment (perpendicular to the surface) of the molecules
20 of liquid crystal. Such slides were used to register a baseline on a UV-Vis-NIR spectrophotometer
21 (SHIMADZU 3600) in the wavelength range 360-3000 nm. After baseline collection, the tested
22 mixtures were applied on the surface of the slide and the spectra were recorded. The measurements
23 were performed in a cooling cycle. The spectrophotometer was equipped with a U7 MLW
24 temperature controller. More details on helical pitch measurements can be found in Ref. [36].
25 Helical pitch length, p , was calculated from the equation $p = \lambda_s/2n_{av}$ for the SmC* phase where λ_s
26 is the wavelength of selectively reflected light from periodic structure and n_{av} is average refractive
27 index (the value of $n_{av} = 1.5$ has been taken for calculation according to Ref. [37]). Dependencies
28 of helical pitch upon temperature are presented.

29 The helix handedness was measured by polarimetry method [38]. The homeotropically
30 aligned sample was observed in transmission between crossed polarizers and the top polarizer was
31 rotated with respect to the bottom one. The analysis of the transmitted light was performed by
32 polarizing optical microscopy (POM). According to the convention described in Ref. [39] a
33 clockwise rotation of analyser, in order to produce the darkest state (or minimum transmission
34 state) when observation is made toward the coming beam, indicates a *dextro* or left-handed helix
35 and anticlockwise rotation indicates a *levo* or right-handed helix. The temperature of the helix twist

1 inversion was established by the analysis of transmitted light versus temperature of a
2 homeotropically aligned sample observed in POM; the brightest texture indicates the fully
3 unwound structure [39].

4 The frequency dispersion of complex permittivity ($\epsilon^* = \epsilon' - i\epsilon''$) has been measured within
5 the temperature range of the SmA* and SmC* phases on cooling, using a Schlumberger 1260
6 impedance analyzer in the frequency range of 1 Hz ÷ 1 MHz keeping the temperature stable during
7 the frequency sweep within ± 0.1 K. The measurements have been performed under zero d.c. bias
8 voltage. The frequency dispersion data have been analysed using the generalized Cole-Cole
9 formula for the frequency dependent complex permittivity extended by the second term to
10 eliminate the low frequency contribution:

$$\epsilon^* - \epsilon_\infty = \frac{\Delta\epsilon}{1 + (jf/f_r)^{(1-\alpha)}} - i \frac{\sigma}{2\pi\epsilon_0 f^n}, \quad (4)$$

11 where f_r is the relaxation frequency, $\Delta\epsilon$ is the dielectric strength, α is the Cole-Cole distribution
12 parameter, ϵ_0 is the permittivity of the vacuum and ϵ_∞ is the high frequency permittivity, σ is the
13 d.c. conductivity and n is a parameter of fitting. The measured real, $\epsilon'(f)$, and imaginary, $\epsilon''(f)$,
14 parts of complex permittivity were fitted simultaneously using specific software “Scientist” from
15 MicroMaths Scientist Software Corporation. For selected representative mixtures, the
16 dependencies of relaxation frequency and dielectric strength upon temperature are presented.
17

18

19 **3. Results and discussion**

20 Here, the description of the multicomponent mixture design together with detailed
21 characterisation of the selected ferroelectric liquid crystalline mixtures are presented. Specifically,
22 the phase diagrams, composition of the best mixtures, together with the spontaneous quantities
23 (namely the spontaneous polarization, tilt angle determined optically, helical pitch length) and
24 dielectric properties for the functional FLC mixtures are shown and discussed.

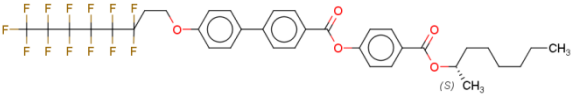
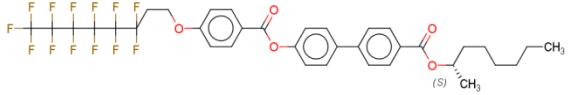
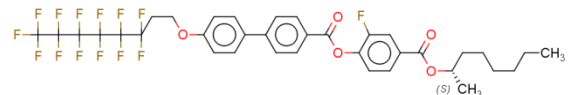
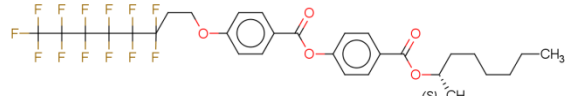
25

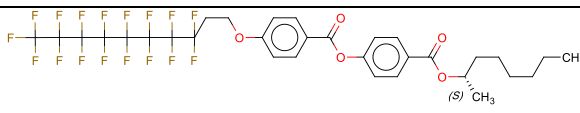
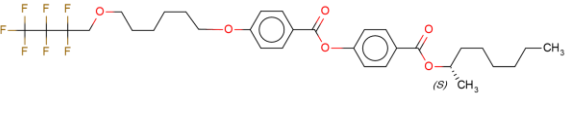
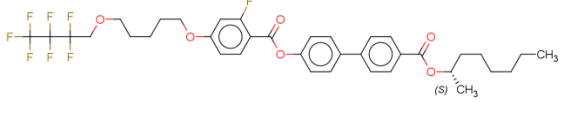
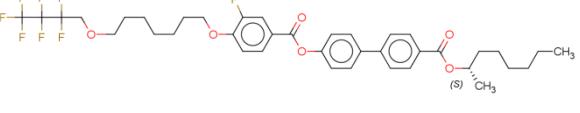
26 **3.1. Mixture design and mesomorphic behaviour**

27 The chemical formulae together with the mesophase sequences and phase transition
28 temperatures on heating cycle of original pure chiral components used for design multicomponent
29 mixtures are presented in Table 1. The precise weight composition of the resulting mixtures is also
30 shown in Table 1. All components possess the same chiral terminal chain; the non-chiral terminal
31 chain differs in number of carbon and fluorine atoms. Other differences are related to the structure
32 of the rigid molecular core. All tested compounds are chiral esters with biphenyl benzoate or
33 phenyl biphenylate, or benzoate rigid core; further tuning of the molecular structure was reached

1 by lateral substitution by fluorine atom at the specific place in the rigid core. Tuning the
 2 concentration of those structurally similar compounds with above mentioned fine differences in
 3 the molecular structure effectively allow us to adjust the required features of resulted designed
 4 multicomponent mixture. Sequence of phases and phase transition temperatures of resulted
 5 multicomponent mixtures are presented and summarised in Table 2.

6
Table 1. Chemical structures, phase transition sequences and temperatures (*in heating cycle*) [°C] of
 chiral components used for design of *W-212B* [33], *W-212C*, *W-212C2* and *W-212C3* mixtures.

No.	Chemical structure and phase sequence of used compounds	Mixtures acronyms			
		<i>W-212B</i>	<i>W-212C</i>	<i>W-212C2</i>	<i>W-212C3</i>
		Concentration (wt%)			
1	 <p>Cr_{II} 80.7°C Cr_I 98.9 °C SmC* 141.4 °C SmC_α* 149.0 °C SmA* 184.0 °C Iso [40-42]</p>	11.88	8.35	7.52	7.52
2	 <p>Cr_{II} 94.3 °C Cr_I 97.9 °C SmC* 155.6 °C SmA* 184.6 °C Iso [40-42]</p>	12.13	8.31	7.48	7.48
3	 <p>Cr 89.7 °C SmC* 133.6 °C SmC_α* 134.8 °C SmA* 154.7 °C Iso [40-42]</p>	24.29	18.54	16.69	16.69
4	 <p>Cr 60.0 °C SmA* 63.4 °C Iso [3]</p>	38.80	29.75	26.77	26.77
5		12.90			

	 <p>Cr 82.2 °C SmA* 90.7 °C Iso [3]</p>				
6	 <p>Cr 36.2 °C Iso [3]</p>	-	35.05	31.54	31.54
7	 <p>Cr 28.1 °C SmC_A* 99.0 °C SmC* 101.0 °C Iso [43]</p>	-	-	10.00	5.25
8	 <p>Cr 37.4 °C SmC_A* 103.1 °C SmC* 104.3 °C SmA* 109.1 °C Iso [43]</p>	-	-	-	4.75

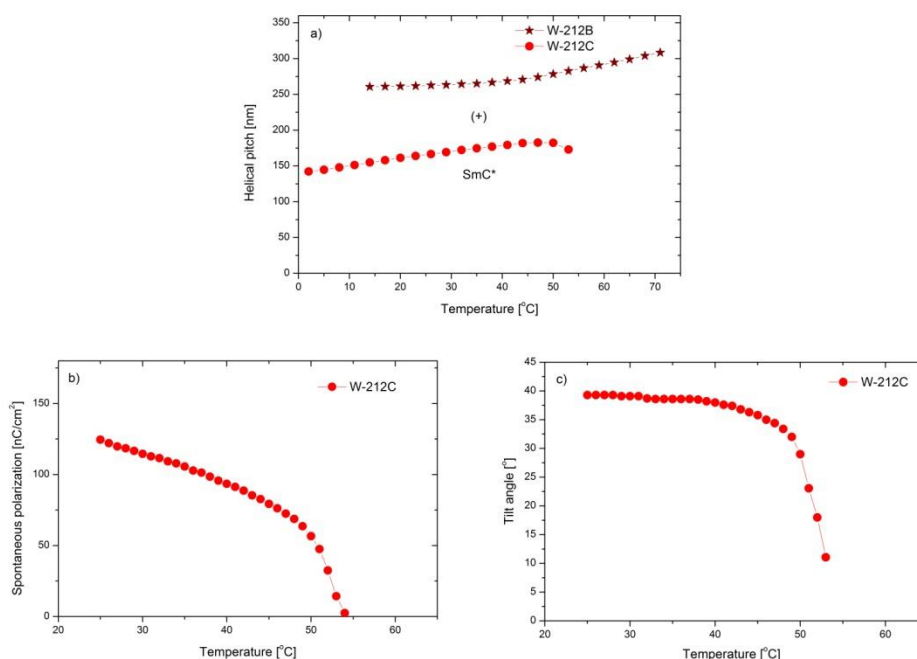
1
2 **Table 2.** Sequence of phases and phase transition temperatures (*on heating cycle*) [°C] for
3 **W-212B** [33], **W-212C**, **W-212C2** and **W-212C3** mixtures.

Mixture	Cr	T	SmC*	T	SmA*	T	Iso
W-212B	●	11.4	●	83.9	●	118.0	●
W-212C	●	<-10.0	●	61.8	●	97.0	●
W-212C2	●	<-10.0	●	61.7	●	71.0	●
W-212C3	●	<-10.0	●	64.4	●	74.7	●

4
5 **3.2. Design and characterization of W-212C mixture**

6 In Ref. [33] the ferroelectric **W-212B** mixture was presented. Its composition is shown in
7 Table 1. It consists of three three-ring esters (compound **1**, **2** and **3**) mixed in proper ratio (1:1:2),
8 respectively. This compounds provide a stable SmC* phase with very high tilt angle value and
9 short helical pitch. Two-ring compounds **4** and **5**, forming the SmA* phase, are added as further
10 functional components in order to decrease the melting temperature of the resulting mixture. This

1 mixture was modified to obtain a material useful for DHF electro-optic effect. The modifications
 2 of **W-212B** mixture presented in Ref. [33] allowed us to decrease considerably the helical pitch
 3 length but at the same time caused too strong increase of the spontaneous polarization (above
 4 $180\text{nC}/\text{cm}^2$ below 30°C). This drawback of mixture **W-212B** motivated our present studies looking
 5 for further improvements. The newly designed **W-212C** mixture was formulated in such a way that
 6 compound **5** was exchanged by a non-mesogenic compound **6**, with much lower melting point and
 7 a strong tendency to decrease helical pitch. Due to that the $\text{SmA}^*-\text{SmC}^*$ phase transition as well
 8 as melting point of **W-212C** mixture is much lower than that of **W-212B** mixture. Furthermore,
 9 and importantly, the helical pitch length has been decreased significantly for **W-212C** mixture in
 10 comparison to **W-212B** as shown in Fig. 1a. The above mentioned results are very consistent with
 11 our previous investigation of miscibility and helical parameters in binary LC systems [3]. Adding
 12 compound **6** to the base compound (in this paper it is compound **I**) results in a slight decrease of
 13 helical pitch value; the SmC^* phase exists up to 0.4 mole fraction of two-ring compound **6** in
 14 binary mixtures. Moderate values of the spontaneous polarization (see Fig. 1b) as well as relatively
 15 high values of the tilt angle (Fig. 1c) are additional important advantages of **W-212C** mixture.



16
 17 **Fig. 1.** Temperature dependence of: (a) the helical pitch length for multicomponent **W-212B** [33]
 18 and **W-212C** mixtures; (b) spontaneous polarization and (c) tilt angle determined optically for
 19 **W212-C** mixture. Sign “+” indicates the right handedness of the helix.

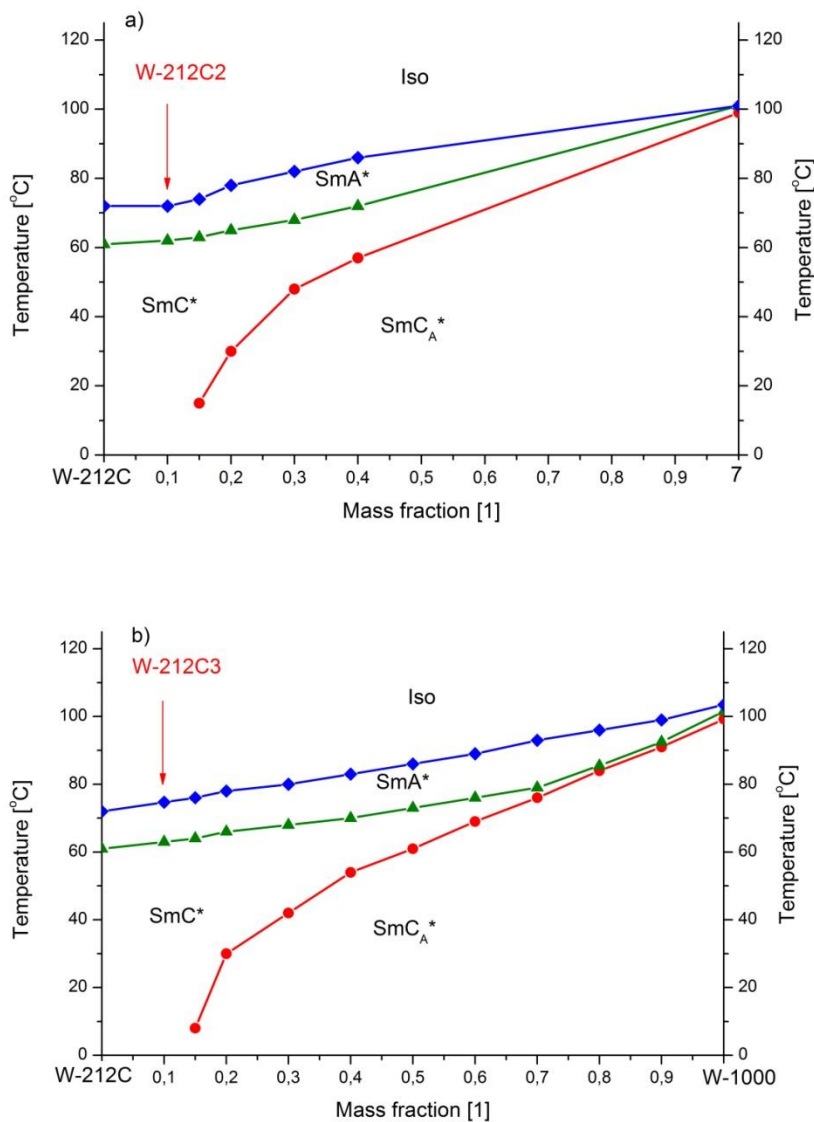
20

21 3.3. Fine tuning of the composition and behaviour of **W-212C** mixture

1 Based on results from our previous work [33], compound **7** and eutectic mixture of
2 compound **7** and **8** (denoted as *W-1000*) were chosen for fine tuning of the behaviour of *W-212C*
3 mixture.

4 Two systems, namely *W-212C* + *compound 7* as well as *W-212C* + *W-1000*, were prepared in
5 order to obtain a proper composition possessing the frustrated ferroelectric phase [34, 35]; this has
6 been done analogically to our previous work [33]. Phase diagrams of those systems are shown in
7 Fig. 2.

8



9

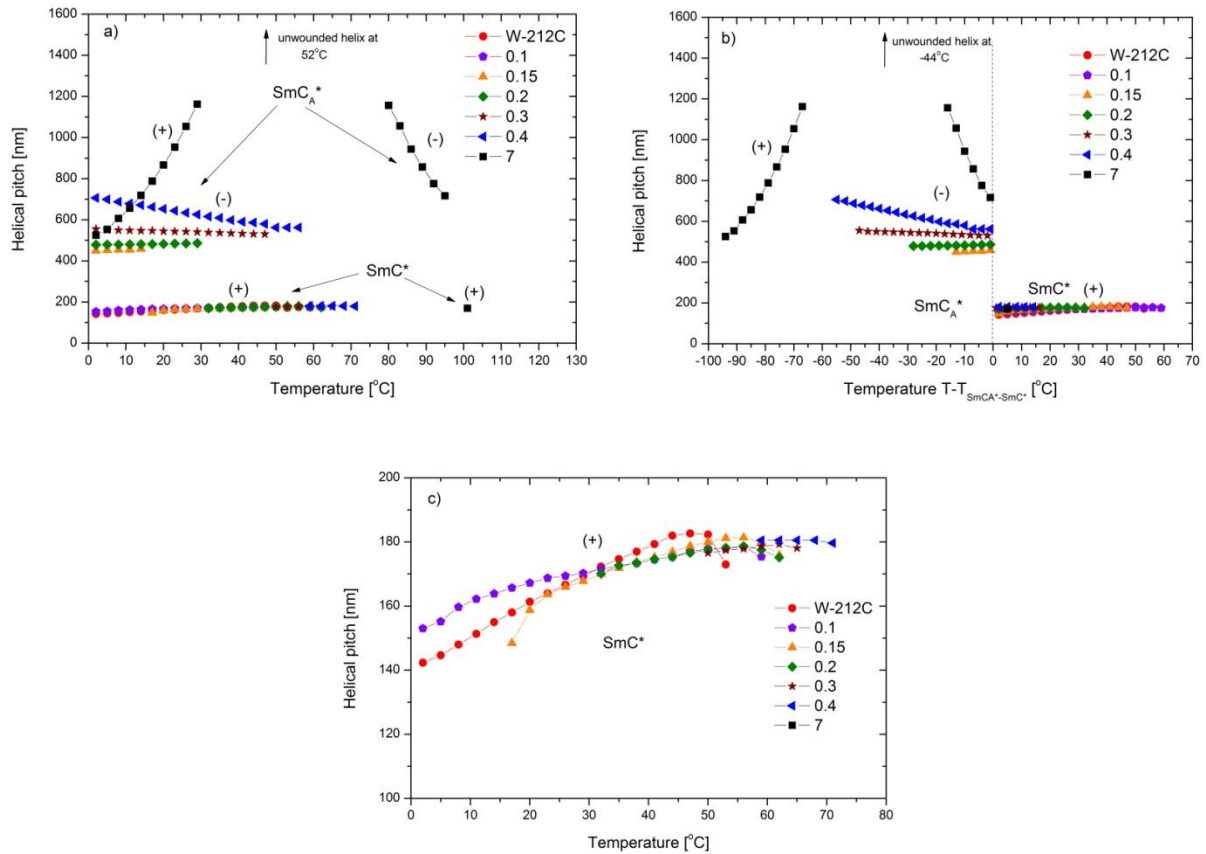
10 **Fig. 2.** Phase diagrams for two systems: (a) *W-212C*+*compound 7* and (b) *W-212C* + *W-1000*.
11 Vertical arrows indicate the specific composition for the resulting *W-212C2* and *W-212C3*
12 mixtures.

13

1 Developed several years ago, *W-1000* mixture is eutectic, bicomponent mixture containing
2 two antiferroelectric compounds (denoted here as **7** and **8**), which possesses on heating the
3 following mesophase sequence: Cr-SmC_A*-SmC*-SmA*-Iso. This mixture is quite highlighted as
4 it exhibits typical orthoconic behaviour which was established recently [44-47]. Whereas *W-212C*
5 mixture is composed from different compounds, namely **1-4** and **6**, as well as it has a similar phase
6 sequence: Cr-SmC*-SmA*-Iso; the antiferroelectric phase is absent. The stability of
7 antiferroelectric phase in system *W-212C+W-1000* is very high (see Fig. 2b) and the
8 destabilization occurs at a very low mass fraction of *W-1000* mixture. System containing up to
9 0.85 mass fraction of *W-212C* mixture still exhibits the antiferroelectric phase at low temperatures.
10 Mixture composition 0.1 + 0.9 mass fraction, for *W-1000* and *W-212C*, respectively, forms the
11 frustrated SmC* phase. In *W-212C+Compound 7* system, the stability of the SmC_A* phase is
12 comparable to the mentioned case (see Fig. 2a). Taking into account the predictions (specifically
13 due to *W-1000* mixture that contains 52.5 wt% of compound **7**) only mixtures containing up to 0.4
14 mass fraction of compound **7** in *W-212C* mixture were prepared. Antiferroelectric phase appears
15 above 0.15 mass fraction of compound **7** in *W-212C* mixture. Similarly, as for the previous system,
16 mixture with 0.1 mass fraction of compound **7** in *W-212C* mixture possesses only the SmC* phase
17 with the broadest temperature range. In comparison to the multicomponent mixtures from *W-212B*
18 series [33], a replacement of one component, which formed the SmA* phase, by another
19 component which does not exhibit any LC behaviour will allow to stabilise the antiferroelectric
20 SmC_A* phase in a much broader concentration range.

21 The results of helical pitch measurements as a function of temperature and of the
22 temperature relative to the SmC*-SmC_A* phase transition obtained for *W-212C + compound 7*
23 and *W-212C+W-1000* systems are given in Fig. 3a and 3b as well as in Fig. 4a and 4b, respectively.
24 In order to compare helical pitch values in the ferroelectric phase, the enlarged areas of the results
25 are shown in Figure 3c and 4c for both systems.

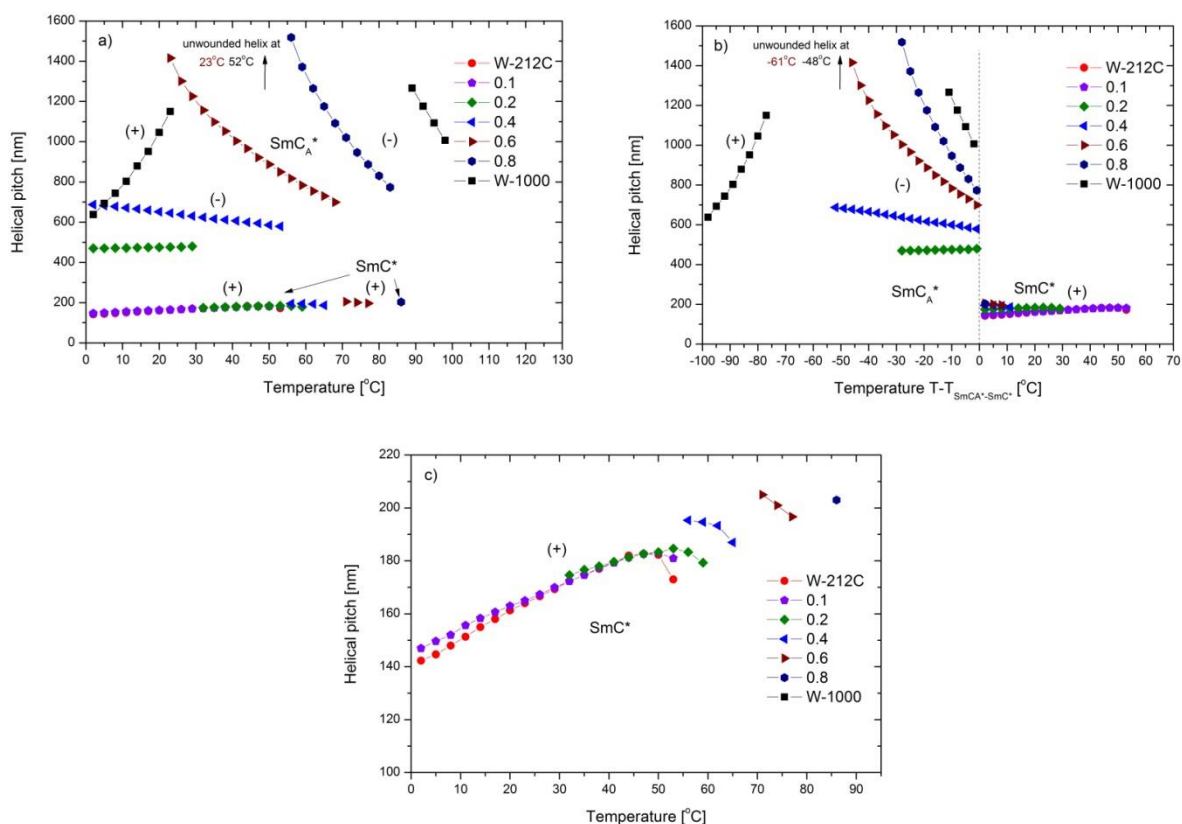
26 Compound **7** is characterized by the presence of right-handed helix in SmC* phase, while in the
27 SmC_A* phase, right and left handedness were observed at the lower and the higher temperature
28 range, respectively (see Fig. 3a). The temperature of helix twist sense inversion of pure compound
29 **7** is equal to 52°C. The multicomponent *W-212C* mixture forms only right-handed helix in the
30 entire temperature range of SmC* phase. Increasing the quantity of compound **7** in *W-212C*
31 mixture causes substantial decrease of helical pitch value for left-handed helix in the SmC_A* phase
32 (see Fig. 3a and 3b). Macroscopic helical structure in the synclinic ferroelectric phase was
33 determined to be right-handed for all mixtures. The lowest value of helical pitch in a broad
34 temperature range was found for *W-212C* mixture containing 0.1 mass fraction of compound **7**.
35 However, *W-212C* mixture possesses the shortest helical pitch below room temperature.



1
 2 **Fig. 3.** Dependence of helical pitch length versus temperature (a) and versus temperature relative
 3 to the SmC^* - SmC_A^* phase transition (b) for $W212C + \text{compound } 7$ system. Enlarged area of the
 4 helical pitch's temperature dependence within the SmC^* phase is shown in (c). Arrows of the
 5 corresponding colour indicate the temperatures at which the helix became fully unwound. The
 6 sense of the helical twist is indicated by “+” for the right-handed helix and by “-“ for the left-
 7 handed helix.

8
 9 The $W-1000$ mixture consists 52.5 wt% of compound 7, therefore its dependence of helical
 10 pitch upon temperature is similar: right handedness at low temperature and left handedness at
 11 higher temperature range of the SmC_A^* phase (see Fig. 4a). Mixtures from system $W-212C + W-$
 12 1000 with 0.15-0.8 mass fractions of $W-1000$ mixture are characterized by the presence of right-
 13 handed helix in the SmC^* phase and left-handed helix in the SmC_A^* phase. The temperatures of
 14 helix twist sense inversion of $W-1000$ mixture as well as of $W-212C$ with 0.8 mass fractions of $W-$
 15 1000 mixture are equal to 52°C and 23°C , respectively. An increase of $W-1000$ mixture
 16 concentration in $W-212C$ mixture causes the appearance of SmC_A^* phase (for 0.15 mass fraction)
 17 and considerable increase of helical pitch for left-handed helix in this phase (see Fig. 4a and 4b).
 18 The helical structure in the ferroelectric phase was found to be right-handed for all compositions.
 19 Both the base $W-212C$ mixture and the $W-212C$ mixture containing 0.1 mass fraction of $W-1000$

1 mixture exhibit the lowest nano-scale values of helical pitch (about 140 nm below room
 2 temperature).
 3



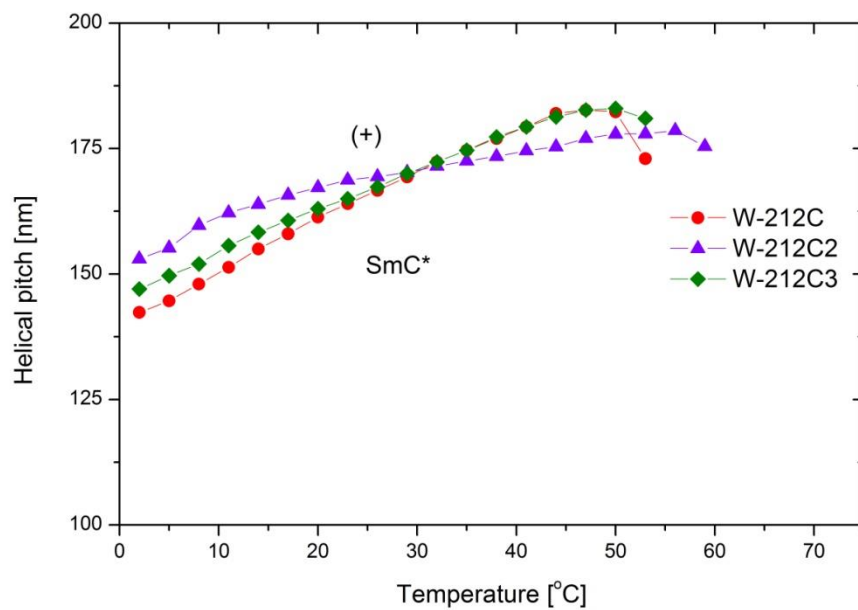
4
 5 **Fig. 4.** Dependence of helical pitch length versus temperature (a) and versus temperature relative
 6 to the SmC*-SmC_A* phase transition (b) for *W-212C* + *W-1000* mixture system. Enlarged area
 7 of temperature dependence of helical pitch in the SmC* phase is shown in (c). Arrows of the
 8 corresponding colour indicate the temperatures at which the helix became fully unwound. The
 9 sense of the helical twist is indicated by “+” for the right-handed helix and by “-” for the left-
 10 handed helix.

11
 12 **3.3. Advanced characterization of resulting *W-212C2* and *W-212C3* mixtures**

13 Base *W-212C* mixture and mixture in which the frustrated ferroelectric phase exists (*W-*
 14 *212C2* and *W-212C3*, marked in red on phase diagrams in Fig. 2a and 2b, respectively) were
 15 chosen for further investigations. Those mixtures possess a quite low melting point (below -10°C),
 16 relatively broad temperature range of the ferroelectric phase (more than 70 degree) and reasonable
 17 temperature range of the paraelectric SmA* phase above the SmC* phase.

18 Temperature dependence of helical pitch length for *W-212C*, *W-212C2* and *W-212C3* mixtures
 19 are shown in Fig. 5 within the SmC* phase. When pure compound 7, which forms left- and right-
 20 handed antiferroelectric phase, is added to the multicomponent ferroelectric *W-212C* mixture, then

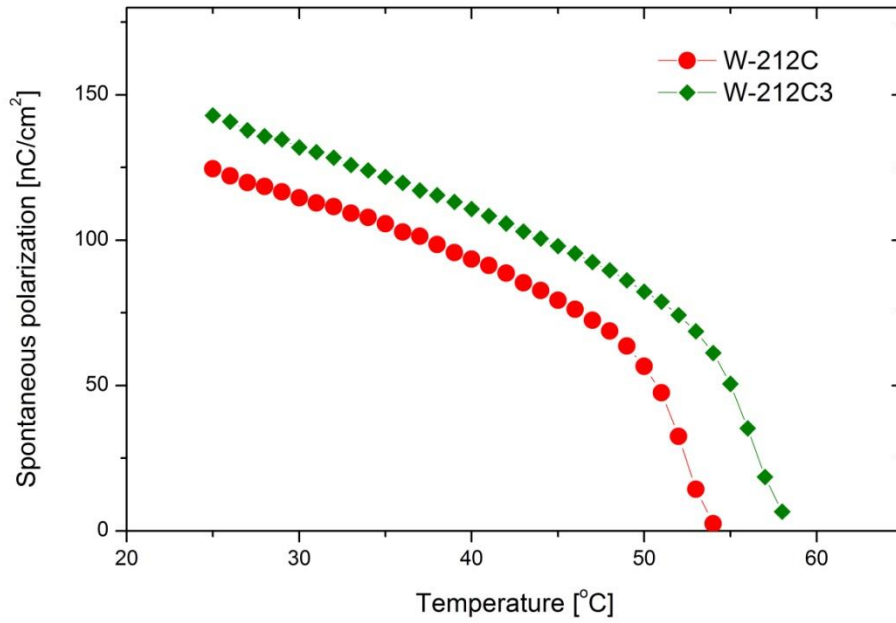
1 the value of helical pitch is decreased in higher temperature region (above 29°C) and increased in
 2 lower temperature region in comparison to values of helical pitch for *W-212C* mixture (see *W-*
 3 *212C2* in Fig. 5). Interestingly, when two compounds **7** and **8** (components of mixture *W-1000*)
 4 are added to *W-212C* mixture, only a slight increase in the length of the helical pitch in low
 5 temperature region is observed (see *W-212C3* in Fig. 5). The value of helical pitch length is lower
 6 than 180 nm for all designed mixtures, although the dependence is slightly growing with
 7 temperature. As the values of helical pitch length for *W-212C2* mixture are the highest from all
 8 three investigated mixtures, further studies were performed for *W-212C* and *W-212C3* mixtures
 9 only.



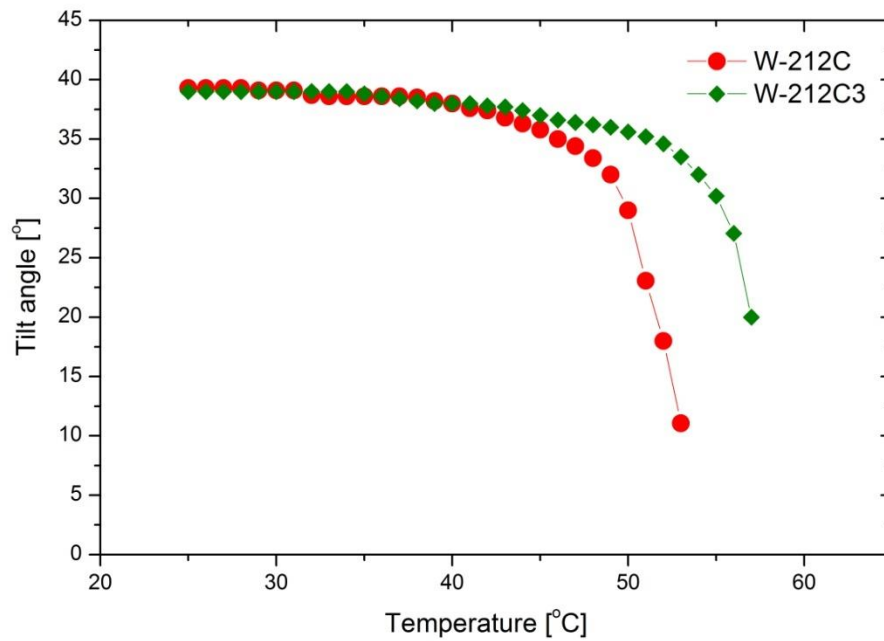
10
 11 **Fig. 5.** Temperature dependence of helical pitch length for *W-212C*, *W-212C2* and *W-212C3*
 12 mixtures as indicated. Sign "+" indicates the right-handedness of the helix.

13
 14 The temperature dependence of the spontaneous polarization $P_s(T)$ and tilt angle $\theta_s(T)$ for
 15 *W-212C* and *W-212C3* mixtures have been measured and are presented in Fig. 6 and Fig. 7,
 16 respectively.

17



1
 2 **Fig. 6.** Temperature dependence of the spontaneous polarization, P_s , for *W-212C* and *W-212C3*
 3 mixtures.
 4



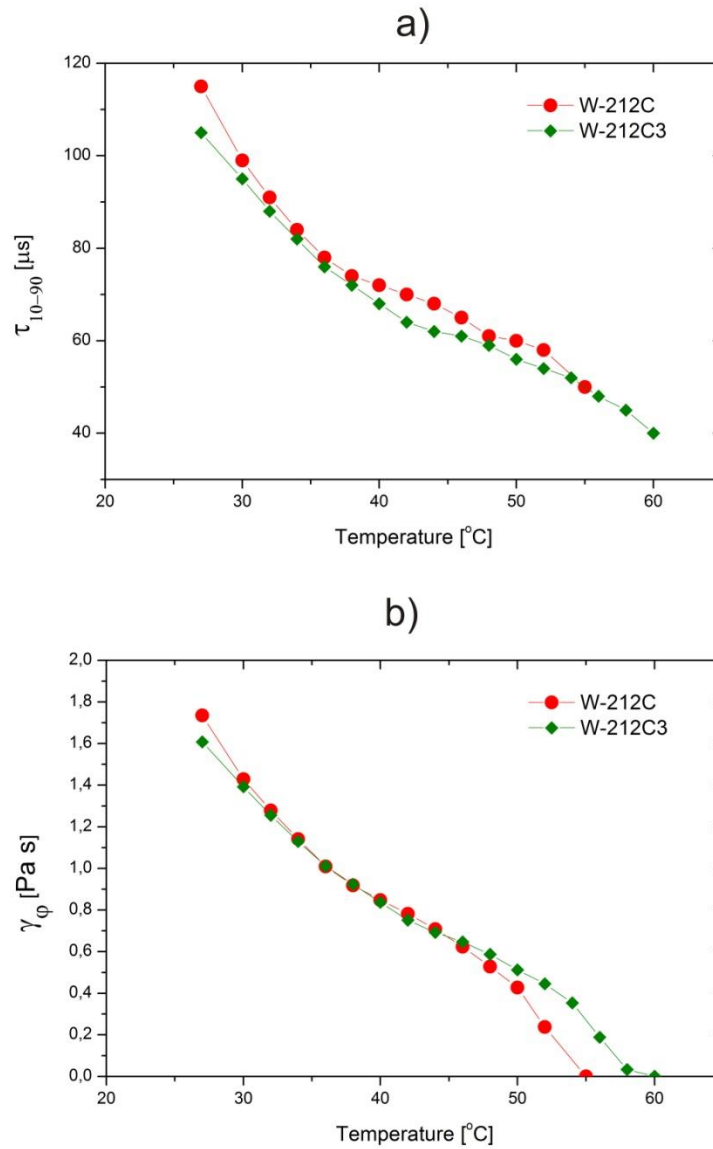
5
 6 **Fig. 7.** Temperature dependence of the tilt angle, θ_s , measured optically for *W-212C* and *W-*
 7 *212C3* mixtures.
 8

1 The lowest value of spontaneous polarization was detected for the base *W-212C* mixture, which
 2 contains the highest quantity of ferroelectric compounds; components with antiferroelectric phase
 3 are absent for this mixture (see Table 1). On the other hand, antiferroelectric components of *W-*
 4 *1000* mixture caused slightly faster saturation of the tilt angle values (about 40 degree) with
 5 temperature decrease in *W-212C3* mixture (Fig. 7).

6 The temperature dependence of the rotational viscosity γ_φ was evaluated from the
 7 measurements of the switching ON time (τ_{10-90}) while driving with a square driving pulse at
 8 saturated voltage (Figure 8a, b). It was calculated using semiempirical formula [48]:

$$9 \quad \gamma_\varphi = \frac{1}{1,8} P_S E \tau_{10-90} \quad (5)$$

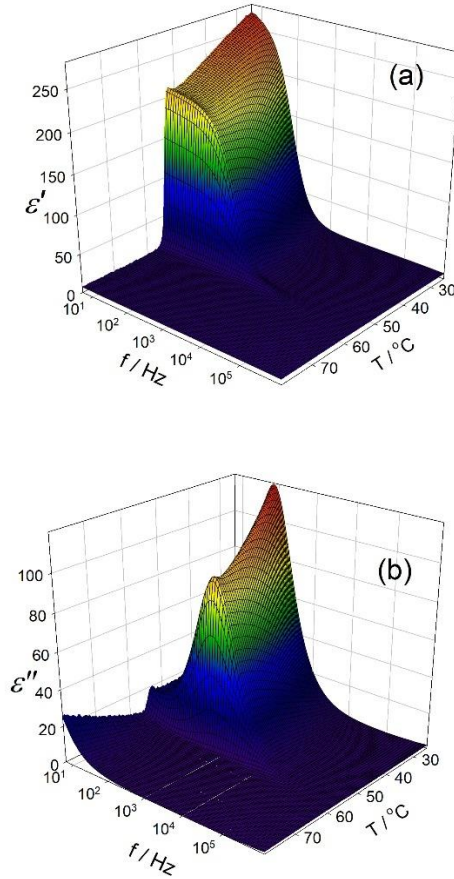
10 where: $E = U/d$, U denotes the applied voltage, d stands for the cell gap.



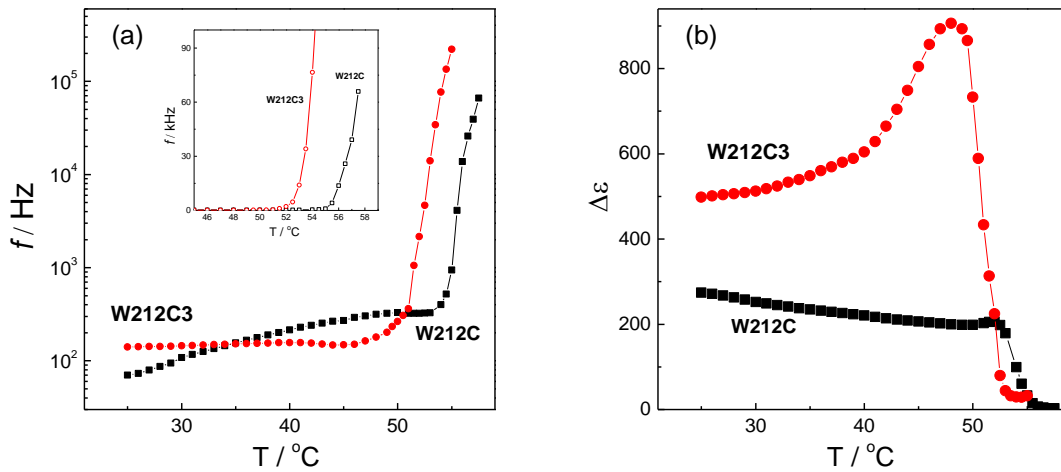
11
 12 **Fig. 8.** Temperature dependence of (a) the switching ON time and (b) the rotational viscosity for
 13 *W212C* and *W212C3* mixtures as indicated.

1 Mixture **W212C** and **W212C3** are characterized by switching On time a little above 100us around
2 room temperature, as it is clear visible in Figure 9a. What is more important for switching times
3 in DHF mode according to the equation (2), both investigated mixtures exhibit rotational viscosity
4 in the range 1 - 1.8 pascal-second. Such values are two times higher than for the newest materials
5 used in DHFLC [31]. However, mixtures **W212C** and **W212C3** exhibit melting points much lower
6 than described in [31].

7 Broadband dielectric spectroscopy was done on two resulting mixtures, namely for **W212C**
8 and **W212C3**. The real, ϵ' , and imaginary parts, ϵ'' , of complex permittivity for **W212C** mixture
9 versus temperature and versus frequency are presented in Figures 9a and 9b as an illustrative result
10 to confirm the ferroelectric character of the polar phase. Dielectric spectra obtained within the
11 whole temperature range of the ferroelectric SmC* phase at zero bias electric field reveal a strong
12 contribution of the Goldstone mode (the relaxation mode related to azimuthal fluctuations of the
13 molecules in the smectic layer). In the vicinity of the SmA*–SmC* phase transition, a collective
14 mode related to the molecular fluctuations in the tilt magnitude, the so-called soft mode, was
15 detected. The measured data were fitted by the Cole-Cole formula (Eq. 4) for the frequency-
16 dependent complex permittivity. The temperature dependence of the fitted relaxation frequency,
17 $f(T)$, and the dielectric increment, $\Delta\epsilon(T)$, are shown in Figs. 10a and 10b for the whole temperature
18 range of the SmA* and SmC* phases. This behaviour fully confirms the ferroelectric character of
19 the SmC* phase detected for the tested mixtures. The relaxation frequency of the mode is slightly
20 decreasing with temperature decrease, while the dielectric strength is continuously decreasing until
21 the crystallisation occurs. This is quite typical behaviour of the Goldstone mode at the ferroelectric
22 SmC* phase [5, 7, 9]. Detailed discussion on the specific behaviour of all detected modes, revealed
23 by the broad-band dielectric spectroscopy, with respect to the mixture composition is beyond the
24 scope of the present work and will be presented elsewhere.



1
 2 **Fig. 9.** 3D-plots of real ε' part (a) and imaginary, ε'' , part (b) of complex permittivity at zero bias
 3 electric field measured on a $12\mu\text{m}$ thick sample cell for *W212C* mixture within the temperature
 4 range of the paraelectric *SmA** and the ferroelectric *SmC** phases.



5
 6 **Fig. 10.** Temperature dependence of (a) the relaxation frequency, $f(T)$, and (b) the dielectric
 7 strength, $\Delta\varepsilon(T)$, at zero applied bias voltage for *W212C* and *W212C3* mixtures as indicated. The
 8 inset in (a) shows the behaviour of the relaxation frequency in the vicinity of the *SmA**-*SmC**
 9 phase transition.

1
2
3
4
5
6
7
8
9
10
11
12
13
14
15
16
17
18
19
20
21
22
23
24
25
26
27
28
29
30
31
32
33
34
35

Conclusions

Three multicomponent mixtures with broad range of the ferroelectric smectic phase, very low melting point, nano-scale helical pitch below 180 nm, high tilt angle and moderate spontaneous polarization have been designed. One of the resulted mixtures is based on compounds possessing the ferroelectric SmC* phase, the orthogonal SmA* phase or without mesophases. Two other mixtures have been developed using the method in which the frustrated ferroelectric phase has been obtained. Such approach gives opportunity to tune the specific features of final mixture by changing the concentration and the type of mixing components as well as unite and even enhance the ferroelectric and antiferroelectric properties of the used components. Furthermore, some mixtures from two designed binary systems (*W212C+W1000* and *W-212C+compound 7*) possess antiferroelectric phase with a very short and simultaneously temperature independent helical pitch that make them potentially useful for deformed helix antiferroelectric liquid crystal (DHAFLC) effect, recently shown by Pozhidaev et al. [49]. Taking into account basic necessities, the designed mixtures fulfilled almost all material requirements for DHF mode, including not too high spontaneous polarization, good chemical stability, due to the absence of the ester group in achiral terminal chain, and compatibility of components, which were the major disadvantages of previously reported *W-212B3A* mixture [33]. However, they exhibit two times higher rotational viscosity but also much lower melting point than the last reported materials for DHF mode [31]. So, that means they can work slower but at lower temperatures. Further work is now underway to investigate in details the electro-optic response of developed mixtures in DHF mode. It is possible to conclude that excellent chemical stability and compatibility of components as well as moderate values of spontaneous polarization adds another great deal to these FLCs mixtures for application in *opto-electronics* and *photonics*.

Acknowledgements

Authors are greatly acknowledged the financial support from the following research projects: Czech Science Foundation CSF 19-03564S, POIG.01.03.01-14-016/08 and PBS 23-895. Two authors (A.B and P.S.) would like to acknowledge also the specific contribution of the COST Action CA17139. Financial support from the grants NKFIH PD 121019 and FK 125134 are acknowledged.

1 **References**

- 2 [1] JPF. Lagerwall, G. Scalia. A new era for liquid crystal research: applications of liquid crystals
3 in soft matter nano-, bio- and microtechnology, *Curr. Appl. Phys.* 2012, 2, 1387-1412.
4 <https://doi.org/10.1016/j.cap.2012.03.019>
- 5 [2] JPF. Lagerwall, F. Giesselmann, Current topics in smectic liquid crystal research, *Chem. Phys.*
6 *Chem.* 2006, 7, 20-45. <https://doi.org/10.1002/cphc.200500472>
- 7 [3] K. Kurp, M. Czerwiński, M. Tykarska, Ferroelectric compounds with chiral (S)-1-
8 methylheptyloxycarbonyl terminal chain – their miscibility and a helical pitch, *Liq. Cryst.*
9 2015, 42(2), 248-254. <https://doi.org/10.1080/02678292.2014.982222>
- 10 [4] Ł. Szczuciński, R. Dąbrowski, S. Urban, K. Garbat, M. Filipowicz, J. Dziaduszek, M.
11 Czerwiński, Synthesis, mesogenic and dielectric properties of fluorosubstituted
12 isothiocyanatoterphenyls, *Liq. Cryst.* 2015, 42, 1706-1729.
13 <https://doi.org/10.1080/02678292.2015.1070924>
- 14 [5] A. Bubnov, V. Novotná, V. Hamplová, M. Kašpar, M. Glogarová, Effect of multilactate chiral
15 part of liquid crystalline molecule on mesomorphic behaviour, *J. Mol. Struct.* 2008, 892, 151-
16 157. <https://doi.org/10.1016/j.molstruc.2008.05.016>
- 17 [6] A. Bubnov, V. Hamplová, M. Kašpar, P. Vaněk, D. Pociecha, M. Glogarová, New ferroelectric
18 liquid crystalline substances with lateral groups in the core, *Mol. Cryst. Liq. Cryst.* 2001, 366,
19 547–556. <https://doi.org/10.1080/10587250108023995>
- 20 [7] V. Novotná, V. Hamplová, A. Bubnov, M. Kašpar, M. Glogarová, N. Kapernaum, S. Bezner,
21 F. Giesselmann, First photoresponsive liquid-crystalline materials with small layer shrinkage
22 at the transition to the ferroelectric phase, *J. Mater. Chem.* 2009, 19, 3992–3997.
23 <https://doi.org/10.1039/b821738f>
- 24 [8] A. Poryvai, A. Bubnov, D. Pociecha, J. Svoboda, M. Kohout, The effect of terminal n-
25 carboxylate chain length on self-assembling and photosensitive properties of lactic acid
26 derivatives, *J. Mol. Liq.* 2019, 275, 829-838. <https://doi.org/10.1016/j.molliq.2018.11.058>
- 27 [9] M. Żurowska, M. Szala, J. Dziaduszek, P. Morawiak, A. Bubnov, Effect of lateral fluorine
28 substitution far from the chiral center on mesomorphic behaviour of highly titled
29 antiferroelectric (S) and (R) enantiomers, *J. Mol. Liq.* 2018, 267, 504-510.
30 <https://doi.org/10.1016/j.molliq.2017.12.114>
- 31 [10] A. Bubnov, V. Hamplová, M. Kašpar, A. Vajda, M. Stojanović, D. Obadović, N. Éber, K.
32 Fodor-Csorba, Thermal analysis of binary liquid crystalline mixtures: system of bent core and
33 calamitic molecules, *J. Therm. Anal. Calori.* 2007, 90, 431-441.
34 <https://doi.org/10.1007/s10973-006-7913-7>

- 1 [11] A. Bubnov, M. Tykarska, V. Hamplová, K. Kurp, Tuning the phase diagrams: the miscibility
2 studies of multilactate liquid crystalline compounds, *Phase Transit.* 2016, 89, 885-893.
3 <https://doi.org/10.1080/01411594.2015.1087523>
- 4 [12] A. Bubnov, N. Podoliak, V. Hamplová, P. Tomášková, J. Havlíček, M. Kašpar, Eutectic
5 behaviour of binary mixtures composed of two isomeric lactic acid derivatives, *Ferroelectrics.*
6 2016, 495, 105-115. <https://doi.org/10.1080/00150193.2016.1136776>
- 7 [13] J. Fitas, M. Marzec, M. Szymkowiak, T. Jaworska-Gołąb, A. Deptuch, M. Tykarska, K. Kurp,
8 M. Żurowska, A. Bubnov, Mesomorphic, electro-optic and structural properties of binary
9 liquid crystalline mixtures with ferroelectric and antiferroelectric liquid crystalline behaviour,
10 *Phase Transit.* 2018, 91, 1017-1026. <https://doi.org/10.1080/01411594.2018.1506883>
- 11 [12] F.V. Podgornov, M. Gavriyak, A. Karaawi, V. Boronin, W. Haase, Mechanism of
12 electrooptic switching time enhancement in ferroelectric liquid crystal/gold nanoparticles
13 dispersion, *Liq. Cryst.* 2018, 45(11), 1594–1602.
14 <https://doi.org/10.1080/02678292.2018.1458256>
- 15 [13] A. Chandran, J. Prakash, KK. Naik, AK. Srivastava, R. Dąbrowski, M. Czerwiński, AM.
16 Biradar, Preparation and characterization of MgO nanoparticles/ferroelectric liquid crystal
17 composites for faster display devices with improved contrast, *J. Mater. Chem. C.* 2014, 2,
18 1844-1853. <https://doi.org/10.1039/c3tc32017k>
- 19 [14] A. Iwan, A. Sikora, V. Hamplová, A. Bubnov, AFM study of advanced composite materials
20 for organic photovoltaic cells with active layer based on P3HT:PCBM and chiral
21 photosensitive liquid crystalline dopants, *Liq. Cryst.* 2015, 42, 964-972.
22 <https://doi.org/10.1080/02678292.2015.1011243>
- 23 [15] RK. Shukla, KK. Raina, V. Hamplová, M. Kašpar, A. Bubnov, Dielectric behaviour of the
24 composite system: multiwall carbon nanotubes dispersed in ferroelectric liquid crystal, *Phase*
25 *Transit.* 2011, 84, 850–857. <https://doi.org/10.1080/01411594.2011.558300>
- 26 [16] A. Bubnov, A. Iwan, M. Cigl, B. Boharewicz, I. Tazbir, K. Wójcik, A. Sikora, V. Hamplová,
27 Photosensitive self-assembling materials as functional dopants for organic photovoltaic cells,
28 *RSC Adv.* 2016, 6, 11577-11590. <https://doi.org/10.1039/C5RA23137J>
- 29 [17] RK. Shukla, A. Chaudhary, A. Bubnov, KK. Raina, Multiwalled carbon nanotubes -
30 ferroelectric liquid crystals nanocomposites: Effect of cell thickness and dopant concentration
31 on electro-optic and dielectric behaviour, *Liq. Cryst.* 2018, 45, 1672-1681.
32 <https://doi.org/10.1080/02678292.2018.1469170>
- 33 [18] N. A. Clark and S. T. Lagerwall, Submicrosecond bistable electro-optic switching in liquid
34 crystals, *Appl. Phys. Lett.* 1980, 36, 899-901. <https://doi.org/10.1063/1.91359>

- 1 [19] A. Bubnov, C. Vacek, M. Czerwiński, T. Vojtylova, W. Piecek, V. Hamplova, Design of polar
2 self-assembling lactic acid derivatives with the keto group and sub-micrometre helical pitch,
3 Beilstein J. Nanotech. 2018, 9, 333-341. <https://doi.org/10.3762/bjnano.9.33>
- 4 [20] V. Swaminathan, V. P. Panov, Yu. P. Panarin, S. P. Sreenilayam, J. K. Vij, A. Panov, D.
5 Rodriguez-Lojo, P. J. Stevenson, E. Gorecka, The effect of chiral doping in achiral smectic
6 liquid crystals on the de Vries characteristics: smectic layer thickness, electro-optics and
7 birefringence, *Liq. Cryst.* 2018, 45(4), 513–521.
8 <https://doi.org/10.1080/02678292.2017.1359694>
- 9 [21] D. Węglowska, P. Perkowski, M. Chronik, M. Czerwiński, The effect of dopant chirality on
10 the properties of self-assembling materials with a ferroelectric order, *Phys. Chem. Chem.*
11 *Phys.* 2018, 20(14), 9211-9220. <https://doi.org/10.1039/c8cp01004h>
- 12 [22] D. Węglowska, P. Perkowski, W. Piecek, M. Mrukiewicz, R. Dąbrowski, The effect of the
13 octan-3-yloxy and the octan-2-yloxy chiral moieties on the mesomorphic properties of
14 ferroelectric liquid crystals, *RSC Adv.* 2016, 5(99), 81003-81012.
15 <https://doi.org/10.1039/c5ra14903g>
- 16 [23] J. Fünfschilling, M. Schadt, Fast responding and highly multiplexible distorted helix
17 ferroelectric liquid-crystal displays, *J. Appl. Phys.* 1989, 66, 3877–3882.
18 <https://doi.org/10.1063/1.344452>
- 19 [24] LA. Beresnev, VG. Chigrinov, DI. Dergachev, EP. Pozhidaev, J. Fünfschilling, M. Schadt,
20 Deformed helix ferroelectric liquid crystal display: a new electrooptic mode in ferroelectric
21 chiral smectic C* liquid crystals, *Liq. Cryst.* 1989, 5, 1171-1177.
22 <https://doi.org/10.1080/02678298908026421>
- 23 [25] I Abdulhalim, G. Moddel, Electrically and optically controlled light modulation and color
24 switching using helix distortion of ferroelectric liquid crystals, *Mol. Cryst. Liq. Cryst.* 1991,
25 200, 79-101. <https://doi.org/10.1080/00268949108044233>
- 26 [26] E. Pozhidaev, S. Torgova, M. Minchenko, C. Augusto Refosco Yednak, A. Strigazzi, E.
27 Miraldi, Phase modulation and ellipticity of the light transmitted through a smectic C* layer
28 with short helix pitch, *Liq. Cryst.* 2010, 37, 1067-1081.
29 <https://doi.org/10.1080/02678292.2010.486482>
- 30 [27] AD. Kiselev, EP. Pozhidaev, VG. Chigrinov, HS. Kwok, Polarization-gratings approach to
31 deformed-helix ferroelectric liquid crystals with subwavelength pitch, *Phys. Rev. E.* 2011, 83,
32 031703. <https://doi.org/10.1103/PhysRevE.83.031703>
- 33 [28] AD. Kiselev, Phase modulation of mixed polarization states in deformed helix ferroelectric
34 liquid crystals, *J. Mol. Liq.* 2018, 267, 253-265. <https://doi.org/10.1016/j.molliq.2017.12.126>

- 1 [29] SP. Kotova, SA. Samagin, EP. Pozhidaev, AD. Kiselev, Light modulation in planar aligned
2 short-pitch deformed-helix ferroelectric liquid crystals, *Phys. Rev. E.* 2015, 92, 062502.
3 <https://doi.org/10.1103/PhysRevE.92.062502>
- 4 [30] VV. Kesaev, AD. Kiselev, EP. Pozhidaev, Modulation of unpolarized light in planar-aligned
5 subwavelength-pitch deformed-helix ferroelectric liquid crystals, *Phys. Rev. E.* 2017, 95,
6 032705. <https://doi.org/10.1103/PhysRevE.95.032705>
- 7 [31] V. Mikhailenko, A. Krivoshey, E. Pozhidaev, E. Popova, A. Fedoryako, S. Gamzaeva, V.
8 Barbashov, AK. Srivastava, HS. Kwok, V. Vashchenko, The nano-scale pitch ferroelectric
9 liquid crystal materials for modern display and photonic application employing highly
10 effective chiral components: Trifluoromethylalkyl diesters of p-terphenyldicarboxylic acid, *J.*
11 *Mol. Liq.* 2019, 281, 186-195. <https://doi.org/10.1016/j.molliq.2019.02.047>
- 12 [32] Q. Guo, Z. Brodzeli, EP. Pozhidaev, F. Fan, VG. Chigrinov, HS. Kwok, L. Silvestri, F.
13 Ladouceur, Fast electrooptical mode in photoaligned reflective deformed helix ferroelectric
14 liquid crystal cells, *Opt. Lett.* 2012, 37(12), 2343-2345.
15 <https://doi.org/10.1364/OL.37.002343>
- 16 [33] K. Kurp, M. Czerwiński, M. Tykarska, A. Bubnov, Design of advanced multicomponent
17 ferroelectric liquid crystalline mixtures with submicrometre helical pitch, *Liq. Cryst.* 2017,
18 44(4), 748-756. <https://doi.org/10.1080/02678292.2016.1239774>
- 19 [34] A. Fukuda, Pretransitional Effect in AF-F Switching: To Suppress It or to Enhance It, That is
20 My Question about AFLCDs, *Proc. 15th Asia Display*, Hamamatsu, 1995 (The Institute of
21 Television Engineers of Japan), Tokyo, 1995, S6-1, 61.
- 22 [35] S. Inui, N. Imura, T. Suzuki, H. Iwane, K. Miyachi, Y. Takanishi, A. Fukuda, Thresholdless
23 antiferroelectricity in liquid crystals and its application to displays, *J. Mater. Chem.* 1996, 6,
24 671-673. <https://doi.org/10.1039/JM9960600671>
- 25 [36] M. Czerwiński, M. Tykarska, Helix parameters in bi- and multicomponent mixtures
26 composed of orthoconic antiferroelectric liquid crystals with three ring molecular core, *Liq.*
27 *Cryst.* 2014, 41(6), 850–860. <https://doi.org/10.1080/02678292.2014.884248>
- 28 [37] Z. Raszewski, J. Kędzierski, P. Perkowski, W. Piecek, J. Rutkowska, S. Kłosowicz, J.
29 Zieliński, Refractive indices of the MHPB(H)PBC and MHPB(F)PBC antiferroelectric liquid
30 crystals, *Ferroelectrics.* 2002, 276, 289-300. <https://doi.org/10.1080/00150190214411>
- 31 [38] W. Kuczyński, ST. Lagerwall, M. Matuszczyk, K. Skarp, B. Stebler, J. Wahl, Fast-switching
32 low-temperature liquid crystal mixture, *Mol. Cryst. Liq. Cryst.* 1987, 146, 173–187.
33 <https://doi.org/10.1080/00268948708071812>

- 1 [39] M. Tykarska, M. Czerwiński, J. Miszkurka, Influence of temperature and terminal chain
2 length on helical pitch in homologue series nH6Bi, *Liq. Cryst.* 2010, 37, 487-495.
3 <https://doi.org/10.1080/02678291003686880>
- 4 [40] W. Drzewiński, K. Czupryński, R. Dąbrowski, M. Neubert, New Antiferroelectric
5 Compounds Containing Partially Fluorinated Terminal Chains. Synthesis and Mesomorphic
6 Properties, *Mol. Cryst. Liq. Cryst.* 1999, 328, 401-410.
7 <https://doi.org/10.1080/10587259908026083>
- 8 [41] P. K. Mandal, B. R. Jaishi, W. Haase, R. Dąbrowski, M. Tykarska, P. Kula, Optical
9 microscopy, DSC and dielectric relaxation spectroscopy studies on a partially fluorinated
10 ferroelectric liquid crystalline compound MHPO(13F)BC, *Phase Transit.* 2006, 79, 223-235.
11 <https://doi.org/10.1080/01411590500500724>
- 12 [42] M. Tykarska, R. Dąbrowski, J. Przedmojski, W. Piecek, K. Skrzypek, B. Donnio, D. Guilon,
13 Physical properties of two systems with induced antiferroelectric phase, *Liq. Cryst.* 2008, 35,
14 1053–1059. <https://doi.org/10.1080/02678290802364004>
- 15 [43] M. Żurowska, R. Dąbrowski, J. Dziaduszek, K. Garbat, M. Filipowicz, M. Tykarska, W.
16 Rejmer, K. Czupryński, A. Spadło, N. Bennis, J.M. Oton, Influence of alkoxy chain length
17 and fluorosubstitution on mesogenic and spectral properties of high tilted antiferroelectric
18 esters, *J. Mater. Chem.* 2011, 21, 2144–2153. <https://doi.org/10.1039/C0JM02015J>
- 19 [44] W. Piecek, P. Perkowski, Z. Raszewski, P. Morawiak, M. Żurowska, R. Dąbrowski, K.
20 Czupryński, Long pitch orthoconic antiferroelectric binary mixture for display applications,
21 *Mol. Cryst. Liq. Cryst.* 2010, 525, 160–172. <https://doi.org/10.1080/15421401003796223>
- 22 [45] M. Czerwiński, M. Tykarska, R. Dąbrowski, A. Chełstowska, M. Żurowska, R. Kowrdziej,
23 L.R. Jaroszewicz, The influence of structure and concentration of cyano-terminated and
24 terphenyl dopants on helical pitch and helical twist sense in orthoconic antiferroelectric
25 mixtures, *Liq. Cryst.* 2012, 39, 1498–1502. <https://doi.org/10.1080/02678292.2012.723047>
- 26 [46] A. Chełstowska, M. Czerwiński, M. Tykarska, N. Bennis, The influence of antiferroelectric
27 compounds on helical pitch of orthoconic W-1000 mixture, *Liq. Cryst.* 2014, 41(6), 812–820.
28 <https://doi.org/10.1080/02678292.2014.885601>
- 29 [47] W. Piecek, A. Bubnov, P. Perkowski, P. Morawiak, K. Ogrodnik, W. Rejmer, M. Żurowska,
30 V. Hamplová, M. Kašpar, An effect of structurally non compatible additive on the properties
31 of a long pitch antiferroelectric orthoconic mixture, *Phase Transit.* 2010, 83, 551-563.
32 <https://doi.org/10.1080/01411594.2010.499496>
- 33 [48] K. Sarp, Rotational viscosities in ferroelectric smectic liquid crystals, *Ferroelectrics.* 1988,
34 84, 119–142. <https://doi.org/10.1080/00150198808016217>

1 [49] E.P. Pozhidaev, V.V. Vashchenko, V. V. Mikhailenko, A.I. Krivoshey, V.A. Barbashov, L.
2 Shi, A.K. Srivastava, V.G. Chigrinov, H.S. Kwok, Ultrashort helix pitch antiferroelectric
3 liquid crystals based on chiral esters of terphenyldicarboxylic acid, *J. Mater. Chem. C*, 2016,
4 4, 10339. <https://doi.org/10.1039/C6TC04087J>
5